

D E C C M A



Working Paper

Validation of Regional Climate Model simulations for the DECCMA project



Ian Macadam, Met Office
Tamara Janes, Met Office



CARIAA
*Collaborative Adaptation Research
Initiative in Africa and Asia*

Citation:

Macadam, I., T. Janes (2017), "Validation of Regional Climate Model simulations for the DECCMA project", DECCMA Working Paper, Deltas, Vulnerability and Climate Change: Migration and Adaptation, IDRC Project Number 107642, www.deccma.com.

About DECCMA Working Papers

This series is based on the work of the Deltas, Vulnerability and Climate Change: Migration and Adaptation (DECCMA) project, funded by Canada's International Development Research Centre (IDRC) and the UK's Department for International Development (DFID) through the **Collaborative Adaptation Research Initiative in Africa and Asia (CARIAA)**. CARIAA aims to build the resilience of vulnerable populations and their livelihoods in three climate change hot spots in Africa and Asia. The program supports collaborative research to inform adaptation policy and practice.

Titles in this series are intended to share initial findings and lessons from research studies commissioned by the program. Papers are intended to foster exchange and dialogue within science and policy circles concerned with climate change adaptation in vulnerability hotspots. As an interim output of the DECCMA project, they have not undergone an external review process. Opinions stated are those of the author(s) and do not necessarily reflect the policies or opinions of IDRC, DFID, or partners. Feedback is welcomed as a means to strengthen these works: some may later be revised for peer-reviewed publication.

Contact

Tamara Janes

Tel: +44 1392 885680

Email: tamara.janes@metoffice.gov.uk

Creative Commons License

This Working Paper is licensed under a Creative Commons Attribution-NonCommercial-ShareAlike 4.0 International License. Articles appearing in this publication may be freely quoted and reproduced provided that i) the source is acknowledged, ii) the material is not used for commercial purposes, and iii) any adaptations of the material are distributed under the same license.

Contents

1. Introduction	2
2. Method	3
3. Results	5
3.1. Results for HadGEM2-ES-forced simulation.....	5
3.2. Results for CNRM-CM5-forced simulation.....	10
3.3. Results for GFDL-CM3-forced simulation.....	14
4. Conclusion	19
Acknowledgements.....	23
References.....	24

1. Introduction

The dynamical downscaling experiments performed for the DECCMA project over south Asia use the PRECIS 2.1 regional climate modelling system, incorporating the HadRM3P Regional Climate Model (RCM). This allows for the downscaling of a number of the Global Climate Models (GCMs) that contributed to the Coupled Model Intercomparison Project phase 5 (CMIP5) (Taylor et al., 2012) to a horizontal resolution of $0.22^\circ \times 0.22^\circ$ (~25km x ~25km). In the DECCMA project, three GCMs (HadGEM2-ES, CNRM-CM5, GFDL-CM3) have been downscaled over the South Asia domain shown in Figure 1 (Janes and Macadam, 2017). A simulation of each of these GCMs has been downscaled between the mid-20th century and late 21st century. This document focuses on the historical period of the RCM downscaling simulations.

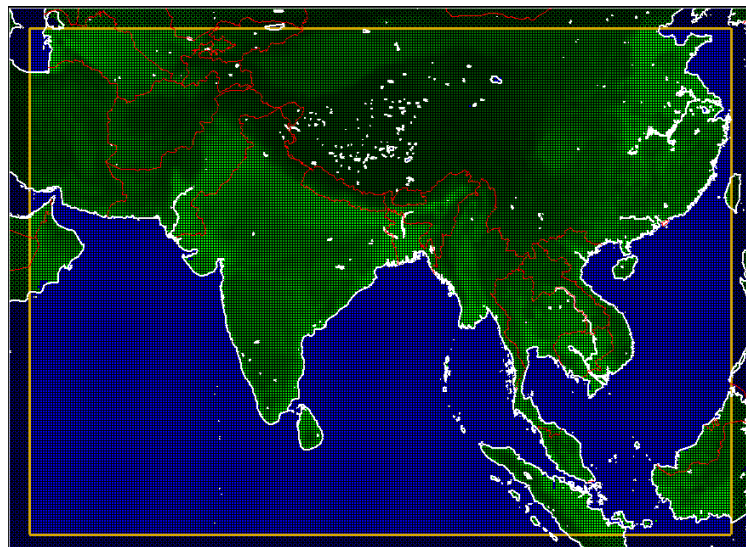


Figure 1: Downscaling domain for South Asia.

This document describes an initial validation of the RCM simulations for the DECCMA project. A brief comparison of RCM output with observational temperature and precipitation datasets is presented. This is designed to inform users of the RCM output about some of the model biases that may be relevant to subsequent analysis of climate impacts. Throughout this document, we refer to differences between RCM output and observational data as “biases”. However, we note that both climate model imperfections and imperfections in observational datasets can contribute to these.

2. Method

Our validation of RCM simulations against climate observations is similar to that of Caesar et al. (2015), who validated PRECIS simulations downscaling the QUMP GCM simulations over Bangladesh and the upstream Ganges, Brahmaputra and Meghna (GBM) river systems. They validated their simulations by comparing them with the gridded observational temperature and precipitation datasets listed in Table 1, and we do likewise. Note that other gridded observational temperature and precipitation datasets are available, but not all of these are suitable for validating RCM simulations. For example, the GPCP and CMAP precipitation datasets (Adler et al., 2003; Xie and Arkin, 1997) have a much coarser spatial resolution than RCM simulations, $2.5^\circ \times 2.5^\circ$.

Dataset	Abbrev.	Variables	Resolution	Period	Reference
Climatic Research Unit TS3.10	CRU	Temperature, Precipitation	$0.5^\circ \times 0.5^\circ$	1901-2009	Harris et al. (2014)
University of Delaware	UDEL	Temperature, Precipitation	$0.5^\circ \times 0.5^\circ$	1950-1999	Willmott & Matsuura (1995)
APHRODITE version 1003R1 dataset (Aph.v10)	APHRODITE	Precipitation	$0.25^\circ \times 0.25^\circ$	1951-2007	Yatagai et al. (2009)
Global Precipitation Climatology Centre	GPCC	Precipitation	$0.5^\circ \times 0.5^\circ$	1901-present	http://gpcc.dwd.de

Table 1: Gridded observational temperature and precipitation datasets used for RCM simulation validation.

Climatological mean surface air temperature and precipitation data for the 1960-1999 period from the RCM simulations and the observed datasets were compared. To aid comparison, all data were regridded to the coarsest of the spatial resolution of the datasets (i.e. regridded onto a $0.5^\circ \times 0.5^\circ$ grid). Further, sea grid cells in the RCM data were masked out to be consistent with the observational datasets, which have no data over the sea.

The RCM and observational data were then compared in two ways. Firstly, the annual cycles in monthly mean data spatially averaged over the common validation region (CVA) shown in Figure 2 were compared. This region covers almost the entire GBM river basin and the entire Mahanadi river basin, both foci of the DECCMA project. However, it also extends further south to include the area of maximum monsoon precipitation from the South Asian Monsoon (SAM), allowing the simulation of the SAM to be assessed. Secondly, maps of climatological mean data for the seasons March-May (MAM), June-September (JJAS), October-November (ON) and December-January (DJF) were compared. For brevity, only the CRU observational datasets were used in this spatially-explicit comparison.

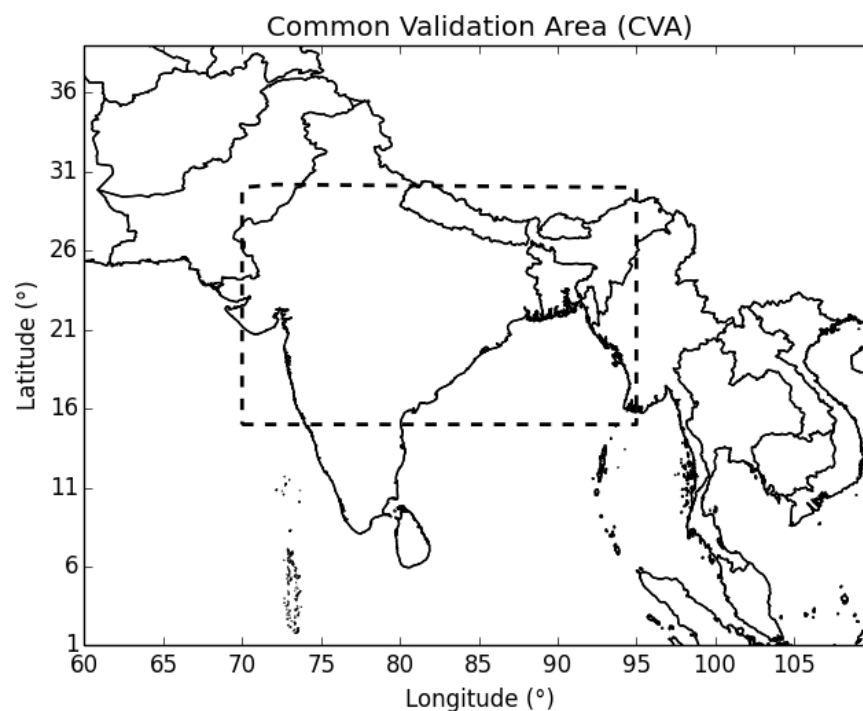


Figure 2: Common Validation Area (bounded by dotted lines) for comparison of annual cycle of RCM and observed temperature and precipitation.

3. Results

3.1. Results for HadGEM2-ES-forced simulation

Figure 3 compares the 1960-1999 climatological mean annual cycles in surface air temperature for the CVA for the HadGEM2-ES-forced RCM simulation and the CRU and UDEL observational datasets. The observational datasets have almost identical annual cycles.

The RCM simulation has a cold bias in CVA-average temperature relative to the observations in all months of the year except May and June. This is most pronounced during the winter months, exceeding 4°C in December and January. The seasonal variation in the magnitude of the bias in CVA-average temperature means that the HadGEM2-ES simulation has a more extreme annual cycle than the annual cycle of the observations. The observed monthly mean CVA-average temperatures vary between approximately 16°C in January and approximately 28.5°C in May. Whereas the maximum monthly mean temperature for the RCM simulation is similar to that of the observations, the simulated minimum monthly mean temperature is approximately 11°C (in January).

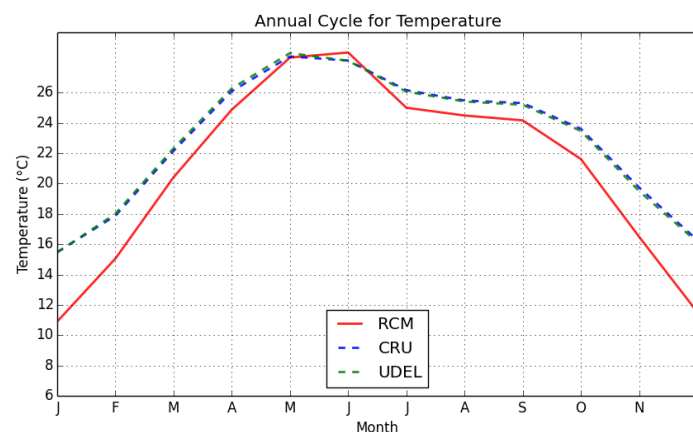


Figure 3: 1960-1999 climatological mean annual cycles in surface air temperature for the CVA for the HadGEM2-ES-forced RCM simulation and the CRU and UDEL observational datasets.

Surface Temperature Comparison (°C):
HadGEM2-ES-forced RCM simulation vs. CRU

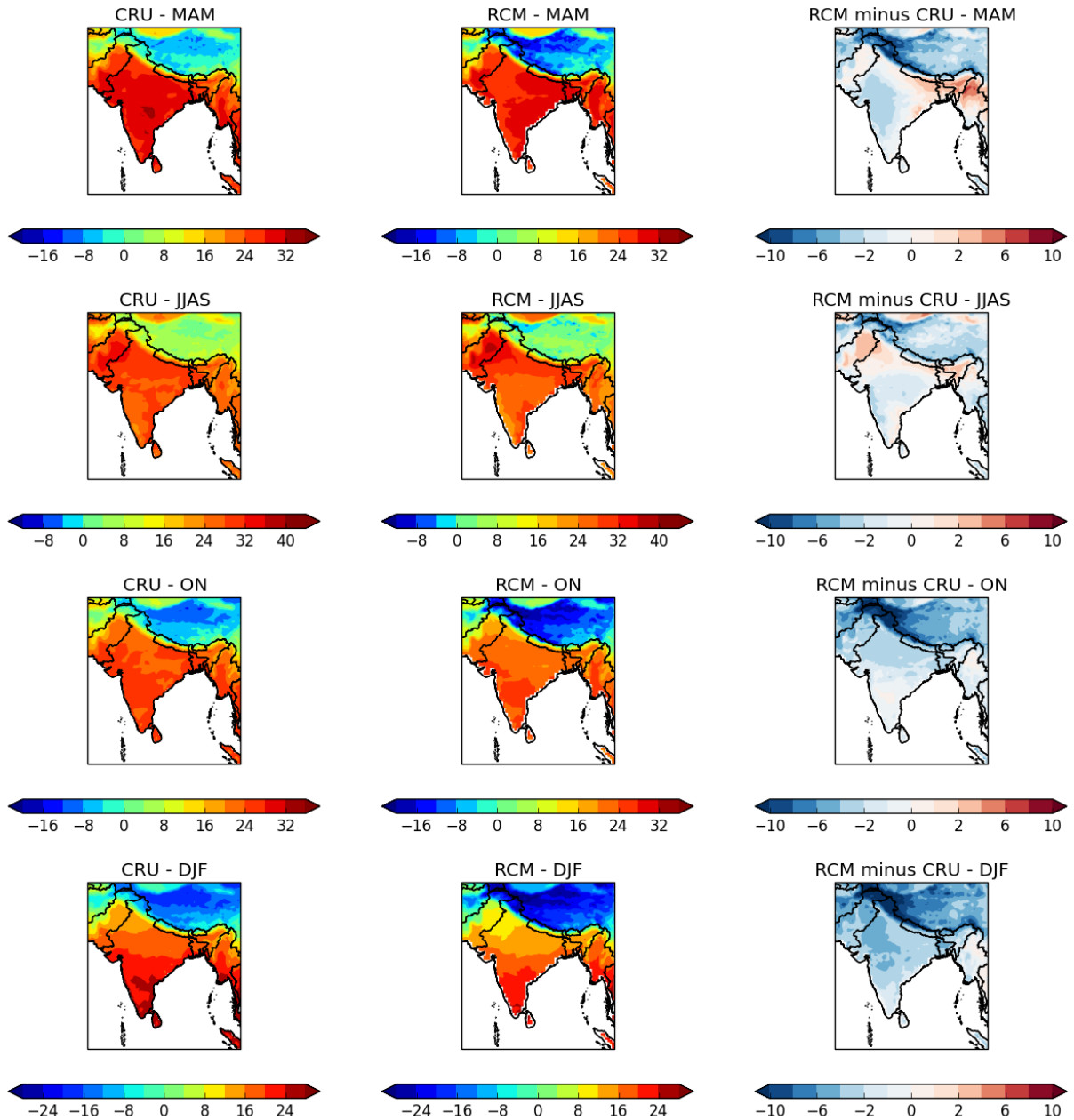


Figure 4: Maps of 1960-1999 climatological mean surface air temperature for March-May (MAM), June-September (JJAS), October-November (ON) and December-January (DJF) for the HadGEM2-ES-forced RCM simulation and the CRU observational dataset. Differences between the RCM and CRU datasets are also shown.

In the winter months, all parts of the CVA have a cold bias (see Figure 4). This appears to be largest in the Himalayas. It is possible that in this topographically complex region differences in elevation between the RCM and the observing sites contributing data to the observational dataset are contributing to this apparent bias. The cold bias in CVA-average temperature is least during the months of the summer monsoon (May to September). In this season, warm biases extend eastwards from Pakistan along the Plain of Ganges and across northern Bangladesh and eastern India and the cold biases that remain within the CVA are smaller than in the winter (see Figure 4).

Figure 5 compares the 1960-1999 climatological mean annual cycles in precipitation for the CVA for the HadGEM2-ES-forced RCM simulation and the CRU, UDEL, GPCC and APHRODITE observational datasets. All four observational datasets all show a distinct winter dry season followed by increasing precipitation through the onset of the summer monsoon in May, to the wettest months in July and August, and then a decline in precipitation. As for temperature, the CRU and UDEL observational datasets have almost identical annual cycles. However, the absolute amount of precipitation differs between the other observational datasets, especially during the wetter months. In these months, the GPCC dataset consistently shows the greatest precipitation and the APHRODITE dataset consistently shows the least precipitation. Such differences between observational datasets have been found in other studies (e.g. Herold et al., 2016). They can arise through different networks of observing stations being used and different methods of interpolating data from the stations onto a spatial grid.

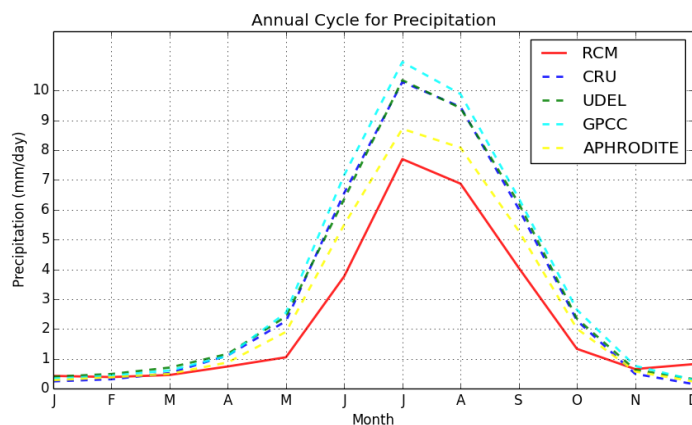


Figure 5: 1960-1999 climatological mean annual cycles in precipitation for the CVA for the HadGEM2-ES-forced RCM simulation and the CRU and UDEL, GPCC and APHRODITE observational datasets.

Rainfall Comparison (mm/day):
HadGEM2-ES-forced RCM simulation vs. CRU

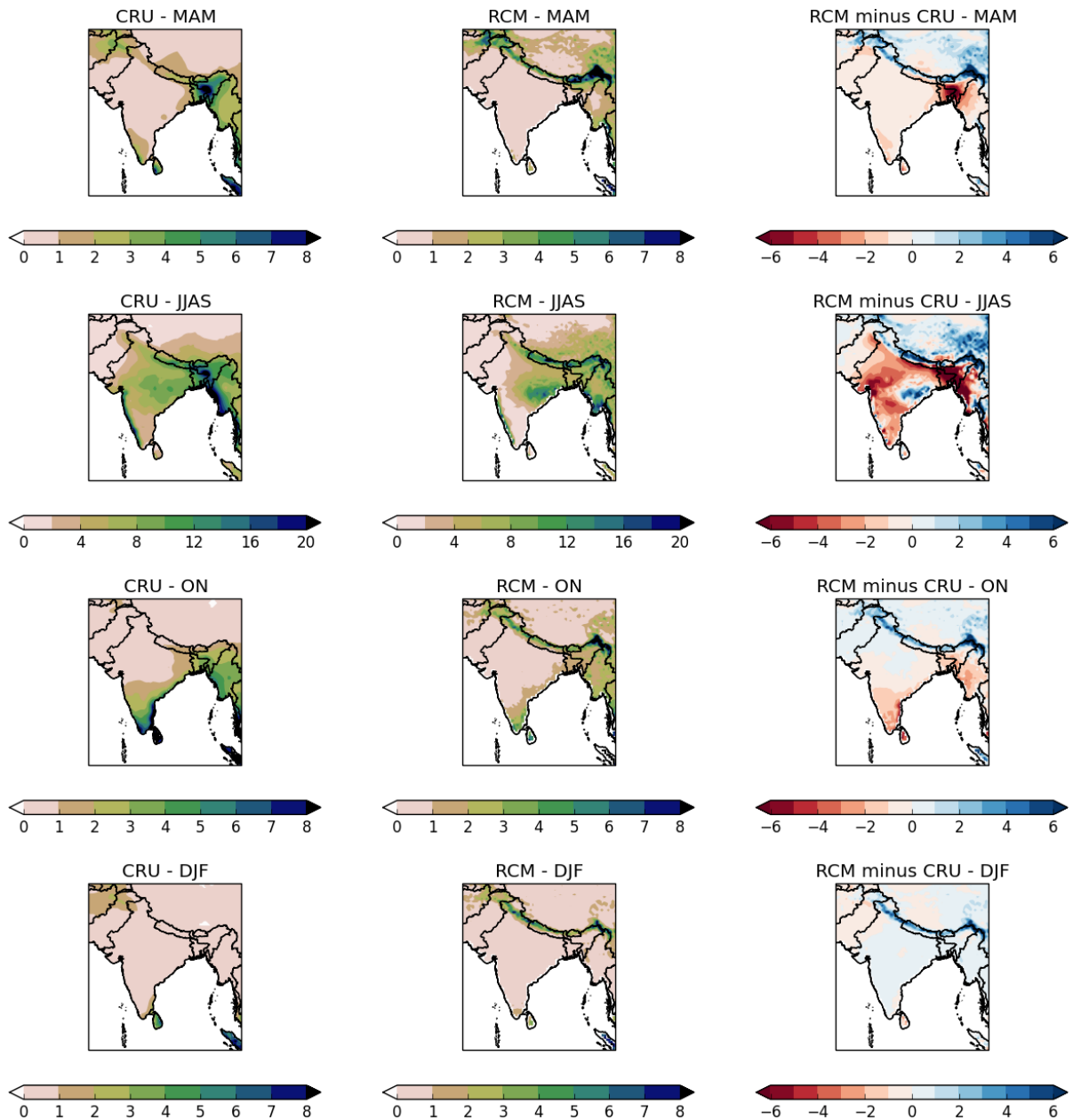


Figure 6: Maps of 1960-1999 climatological mean precipitation for March-May (MAM), June-September (JJAS), October-November (ON) and December-January (DJF) for the HadGEM2-ES-forced RCM simulation and the CRU observational dataset. Differences between the RCM and CRU datasets are also shown.

The HadGEM2-ES-forced RCM simulation reproduces the annual cycle in CVA-average precipitation but has a dry bias relative to all of the observational datasets throughout the summer monsoon. During the build-up and decline of the monsoon in the March-May and October-November seasons, dry biases of more than 2mm/day within the CVA are largely confined to Bangladesh and eastern India (see Figure 6). However, in the June-September season, when the dry bias in CVA-average precipitation is largest, dry biases of this magnitude extend across much of India and Bangladesh, though are largest in Bangladesh and eastern India. Throughout the year, dry biases are partially offset by wet biases in the Himalayas. Wet biases in the Himalayas throughout the year appear to be a common feature of other HadRM3P simulations of the region (see Sections 3.2 and 3.3 and Caesar et al., 2005). At least some of these apparent wet biases in the Himalayas could be due to underrepresentation of precipitation in the observational data. One contributory factor could be that at high altitudes “undercatch” of precipitation by rain gauges can be particularly pronounced due to precipitation falling as snow. Some studies have attempted to address this issue by applying undercatch corrections to observational precipitation datasets, and a greater correction is required for snow than for rainfall (e.g. Weedon et al., 2010).

3.2. Results for CNRM-CM5-forced simulation

Figure 7 compares the 1960-1999 climatological mean annual cycles in surface air temperature for the CVA for the CNRM-CM5-forced RCM simulation and the CRU and UDEL observational datasets. The CNRM-CM5-forced simulation has a similar annual cycle, and range in monthly mean CVA-average temperatures, to the HadGEM2-ES-forced simulation (see Figure 3), but has an additional cold bias of approximately 1°C. Hence the CNRM-CM5-forced simulation has a 1°C cold bias even in May and June, in which the HadGEM2-ES-forced simulation has minimal bias, and the largest biases in the CNRM-CM5-forced simulation, for December and January, exceed 5°C.

The spatial patterns of cold biases for the CNRM-CM5-forced simulation (see Figure 8) are similar to those for the HadGEM2-ES-forced simulation (see Figure 4), with the largest biases being located in the Himalayas. However, the cold biases in the CNRM-CM5-forced simulation are generally larger than the cold biases in the HadGEM2-ES-forced simulation. Another difference between the two simulations is that in the CNRM-CM5-forced simulation warm biases of more than 1°C are largely confined to Bangladesh and eastern India in the March-May season. Unlike in the HadGEM2-ES-forced simulation, warm biases during the height of the summer monsoon (June to September) are minimal, which contributes to the larger cold bias in CVA-average temperature in the CNRM-CM5-forced simulation than in the HadGEM2-ES-forced simulation in this season.

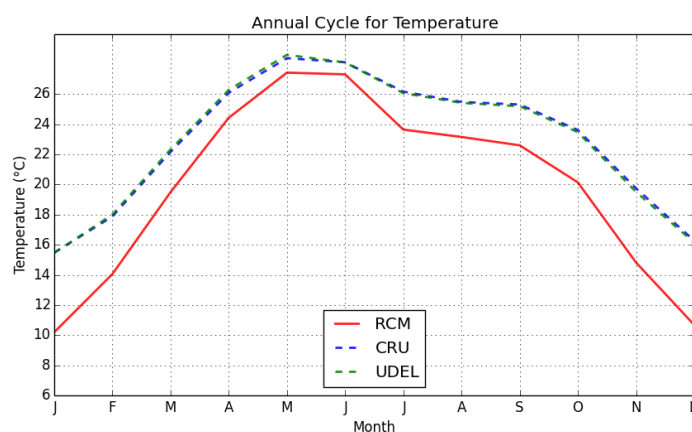


Figure 7: 1960-1999 climatological mean annual cycles in surface air temperature for the CVA for the CNRM-CM5-forced RCM simulation and the CRU and UDEL observational datasets.

Surface Temperature Comparison (°C):
CNRM-CM5-forced RCM simulation vs. CRU

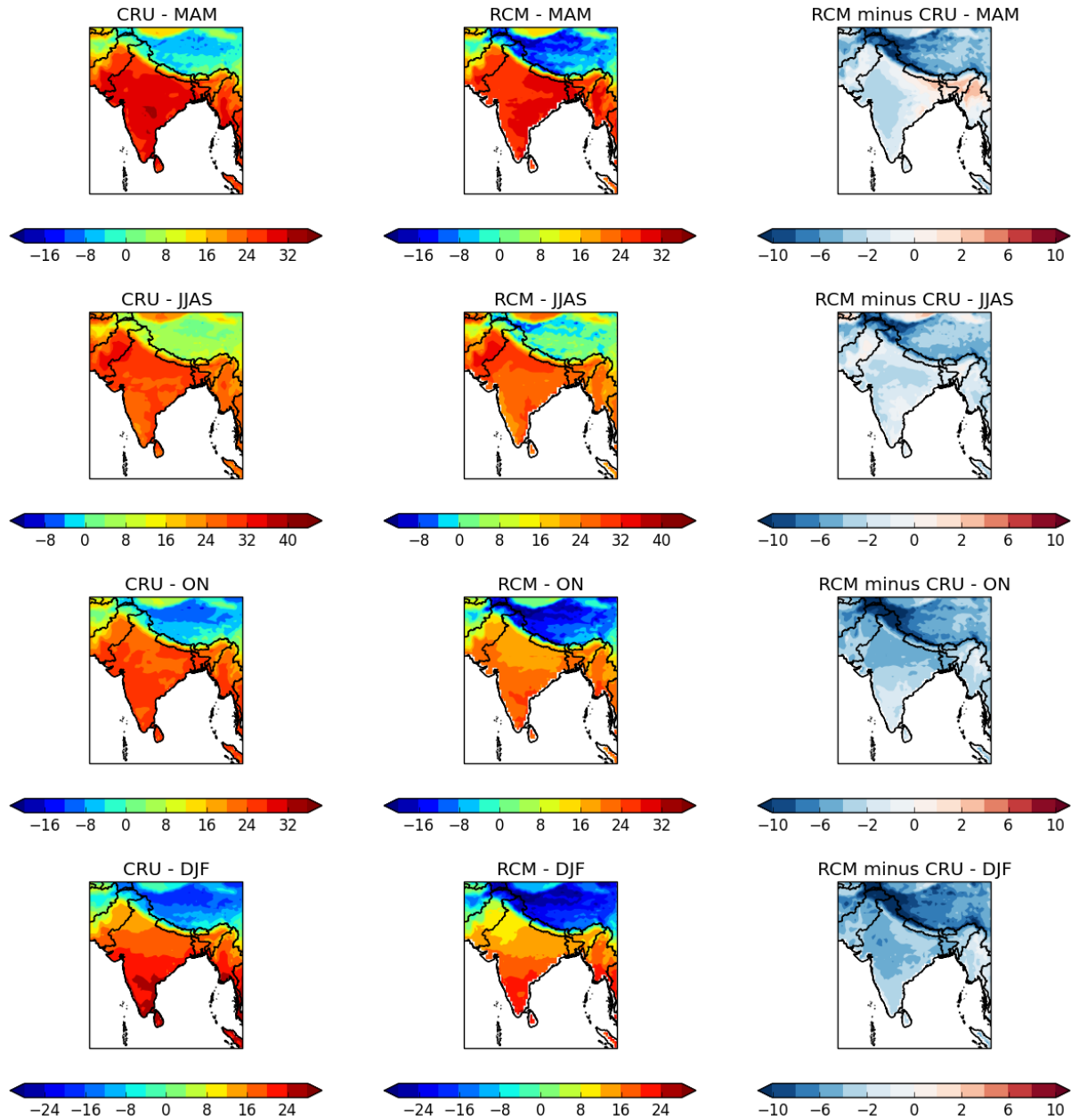


Figure 8: Maps of 1960-1999 climatological mean surface air temperature for March-May (MAM), June-September (JJAS), October-November (ON) and December-January (DJF) for the CNRM-CM5-forced RCM simulation and the CRU observational dataset. Differences between the RCM and CRU datasets are also shown.

Figure 9 compares the 1960-1999 climatological mean annual cycles in precipitation for the CVA for the CNRM-CM5-forced RCM simulation and the CRU, UDEL, GPCC and APHRODITE observational datasets. As for the HadGEM2-ES-forced simulation, the CNRM-CM5-forced simulation reproduces the annual cycle in CVA-average precipitation. However, in contrast to the HadGEM2-ES-forced simulation, for the wetter months, the simulated CVA-average precipitation lies within the observational uncertainty described by the four observational datasets. For these months, the simulated CVA-average precipitation values are between those of the GPCC and APHRODITE datasets, and, except for in July and August, similar to those of the CRU and UDEL datasets.

The spatial patterns of precipitation biases in the CNRM-CM5-forced simulation (see Figure 10) are similar to those in the HadGEM2-ES-forced simulation (see Figure 6), with wet biases in the Himalayas throughout the year and the largest dry biases in the CVA in Bangladesh and eastern India during the June-September summer monsoon season. However, the dry biases in this season are much less extensive than in the HadGEM2-ES-forced simulation, which contributes to the better match between the simulated and observed CVA-average precipitation values for the CNRM-CM5-forced simulation than for the HadGEM2-ES-forced simulation.

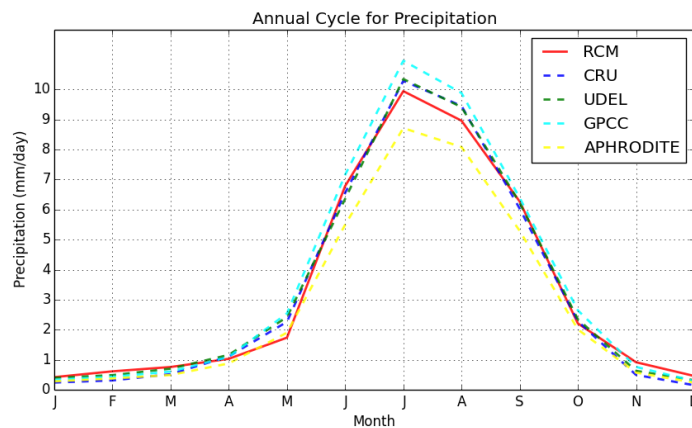


Figure 9: 1960-1999 climatological mean annual cycles in precipitation for the CVA for the CNRM-CM5-forced RCM simulation and the CRU and UDEL, GPCC and APHRODITE observational datasets.

Rainfall Comparison (mm/day): CNRM-CM5-forced RCM simulation vs. CRU

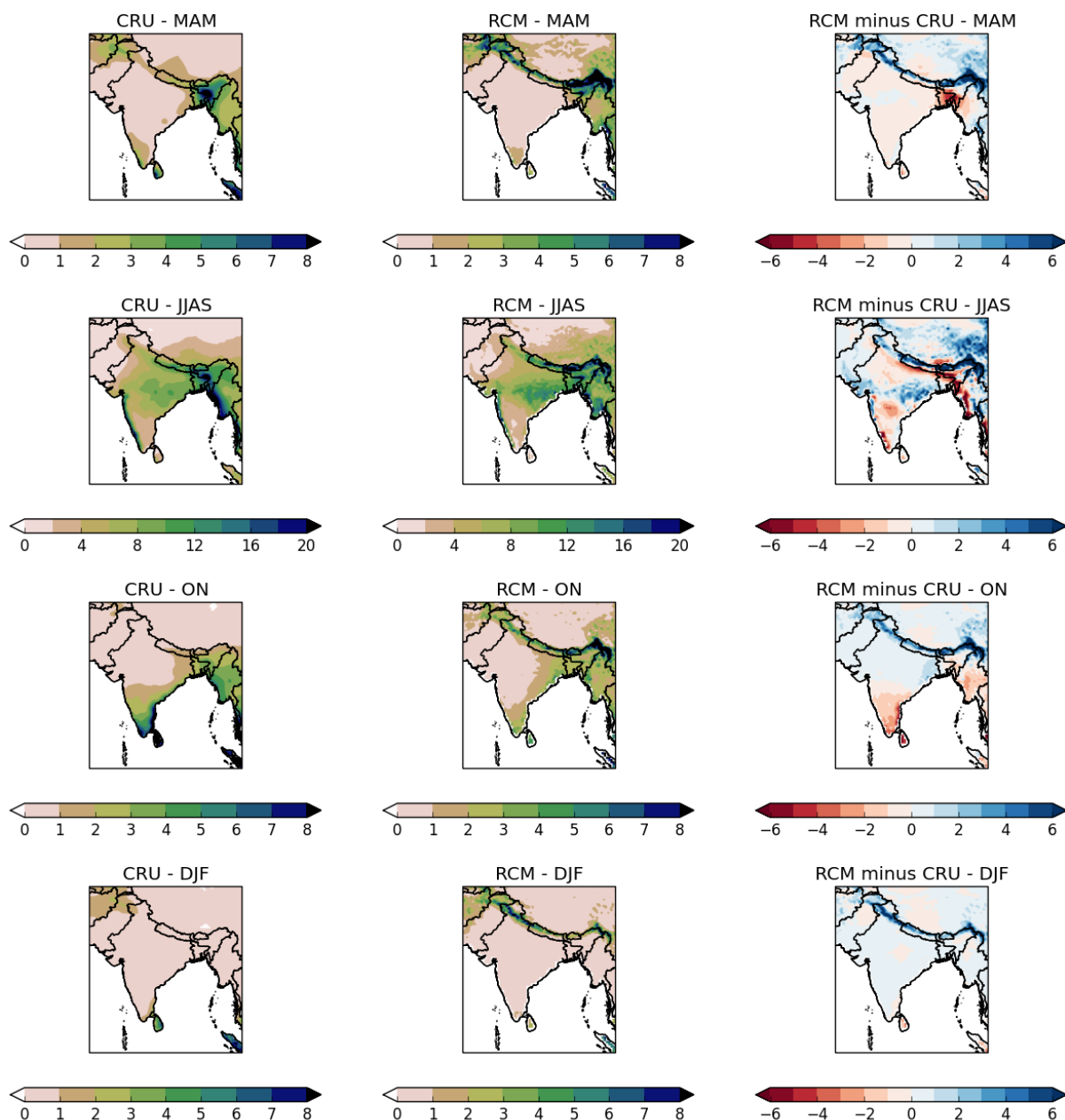


Figure 10: Maps of 1960-1999 climatological mean precipitation for March-May (MAM), June-September (JJAS), October-November (ON) and December-January (DJF) for the CNRM-CM5-forced RCM simulation and the CRU observational dataset. Differences between the RCM and CRU datasets are also shown.

3.3. Results for GFDL-CM3-forced simulation

Figure 11 compares the 1960-1999 climatological mean annual cycles in surface air temperature for the CVA for the GFDL-CM3-forced RCM simulation and the CRU and UDEL observational datasets. The GFDL-CM3-forced simulation has a more extreme annual cycle than the annual cycle of the observations, and the HadGEM2-ES-forced and CNRM-CM5-forced simulations. Whereas the observed monthly mean CVA-average temperatures vary between approximately 16°C in January and approximately 28.5°C in May, the monthly mean temperatures from the GFDL-CM3-forced simulation vary between approximately 10°C in January and 29°C in June. Hence there is a pronounced cold bias in the winter months of the year, which exceeds 6°C in January. In addition, June is significantly warmer, by about 1.5°C than May, the second warmest month. May and June have approximately the same monthly mean temperatures in the observations, and in the HadGEM2-ES-forced and CNRM-CM5-forced simulations.

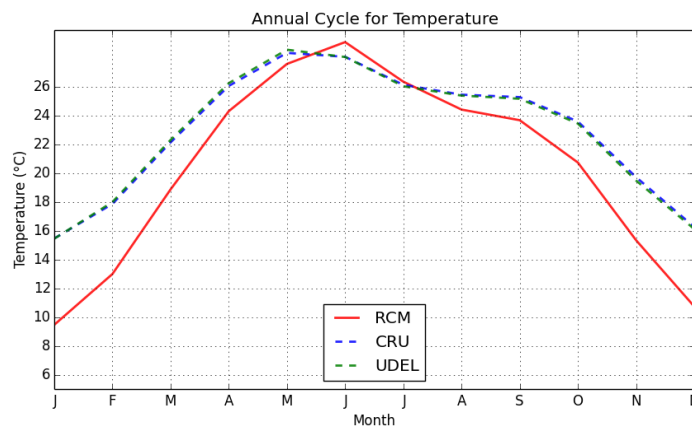


Figure 11: 1960-1999 climatological mean annual cycles in surface air temperature for the CVA for the GFDL-CM3-forced RCM simulation and the CRU and UDEL observational datasets.

Surface Temperature Comparison (°C):
GFDL-CM3-forced RCM simulation vs. CRU

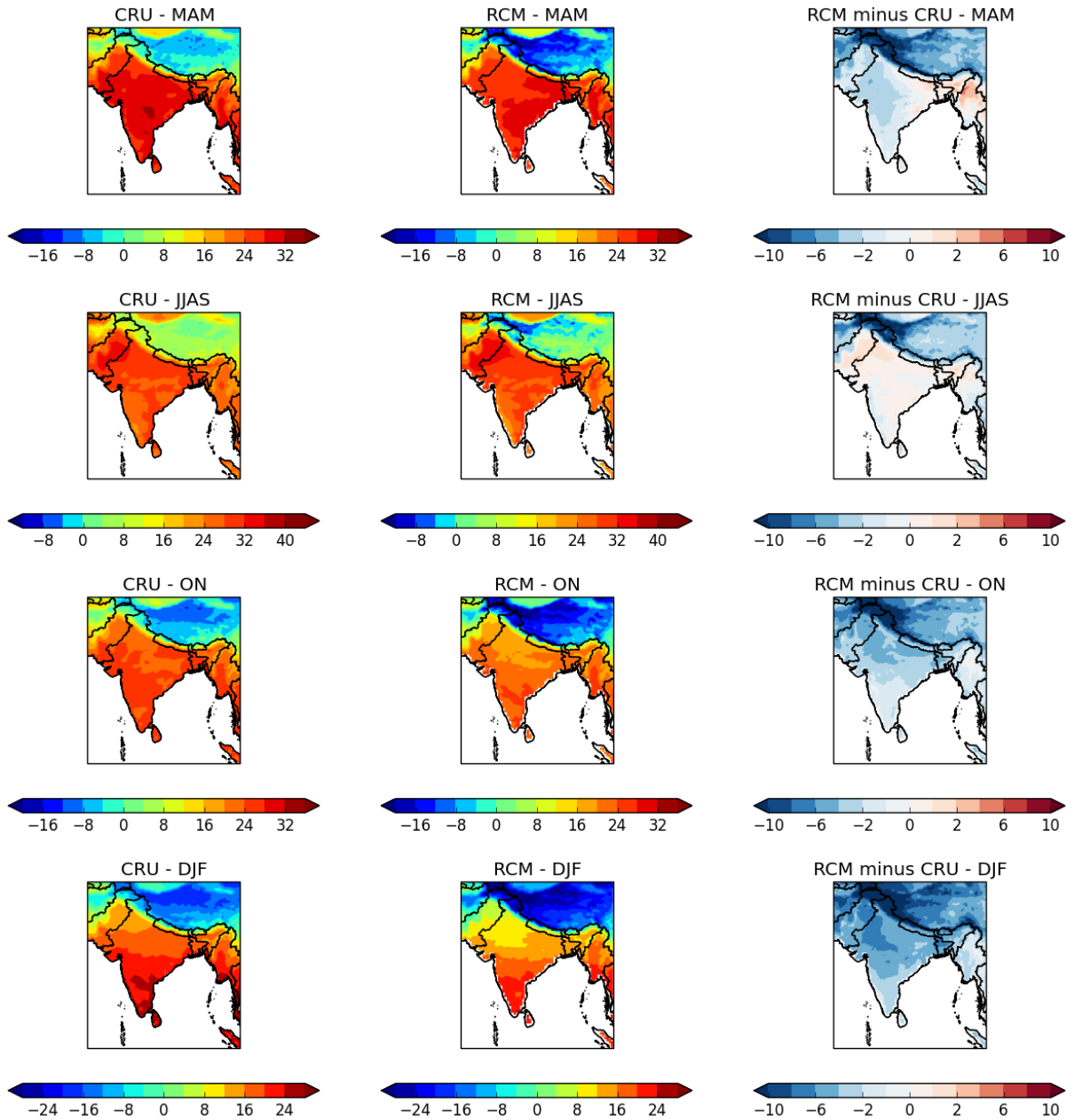


Figure 12: Maps of 1960-1999 climatological mean surface air temperature for March-May (MAM), June-September (JJAS), October-November (ON) and December-January (DJF) for the GFDL-CM3-forced RCM simulation and the CRU observational dataset. Differences between the RCM and CRU datasets are also shown.

Outside the height of the summer monsoon (June-September), the spatial patterns of cold biases in the GFDL-CM3-forced simulation (see Figure 12) are similar to those in the HadGEM2-ES-forced and CNRM-CM5-forced simulations (see Figures 4 and 8), with the largest biases being located in the Himalayas. However, in winter, the cold biases in the GFDL-CM3-forced simulation are generally larger than the cold biases in the HadGEM2-ES-forced simulation and, to a lesser extent, those in the CNRM-CM5-forced simulation. This results in the larger cold bias in CVA-average temperature in the GFDL-CM3-forced simulation than in the HadGEM2-ES-forced simulation and, to a lesser extent, than in the CNRM-CM5-forced simulation in this season. During June-September, temperature biases across most of the CVA are minimal, although cold biases persist in the Himalayas. Hence the bias in CVA-average temperature is small for this season.

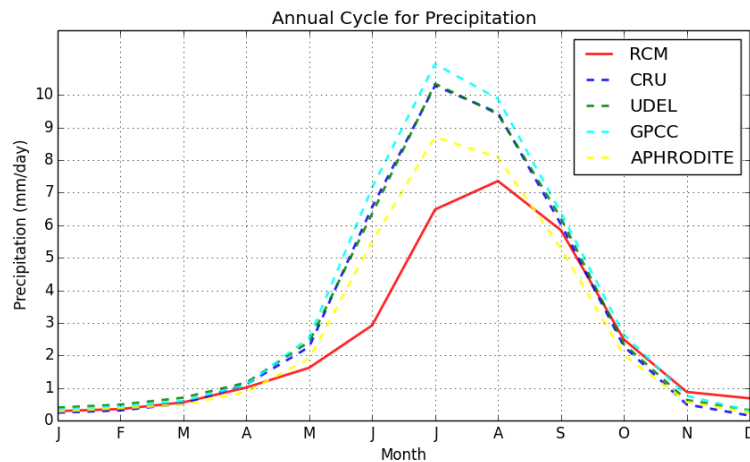


Figure 13: 1960-1999 climatological mean annual cycles in precipitation for the CVA for the GFDL-CM3-forced RCM simulation and the CRU and UDEL, GPCP and APHRODITE observational datasets.

Figure 13 compares the 1960-1999 climatological mean annual cycles in precipitation for the CVA for the GFDL-CM3-forced RCM simulation and the CRU, UDEL, GPCP and APHRODITE observational datasets. As for the HadGEM2-ES-forced simulation, the GFDL-CM3-forced simulation has an overall dry bias in CVA-average precipitation relative to all four observational datasets. However, unlike both the HadGEM2-ES-forced and CNRM-CM5-forced simulations, the maximum monthly mean precipitation is later in the GFDL-CM3-forced simulation than in the observations. The maximum monthly mean precipitation occurs in July in all four observational datasets and the HadGEM2-ES-

forced and CNRM-CM5-forced simulations, whereas it occurs in August for the GFDL-CM3-forced simulation. The simulated monthly mean CVA-average precipitation values match the observations well in September and October. It is possible that there is a dry bias in the simulation during the build up to the monsoon and the monsoon itself, but not during the monsoon decay. Alternatively, the monsoon rains could be delayed in the simulation relative to the observations and this effect cancels out an overall dry bias to give unbiased monthly mean precipitation values for September and October. A comparison of the simulated and observed monsoon circulation would be necessary to test these hypotheses.

The spatial patterns of precipitation biases in the GFDL-CM3-forced simulation (see Figure 14) are similar to those in the HadGEM2-ES-forced simulation (see Figure 6), with wet biases in the Himalayas throughout the year and the largest dry biases in the CVA in Bangladesh and eastern India during the June to September summer monsoon season. However, the extent of the dry biases in India in this season is even greater than in the HadGEM2-ES-forced simulation.

Rainfall Comparison (mm/day):
GFDL-CM3-forced RCM simulation vs. CRU

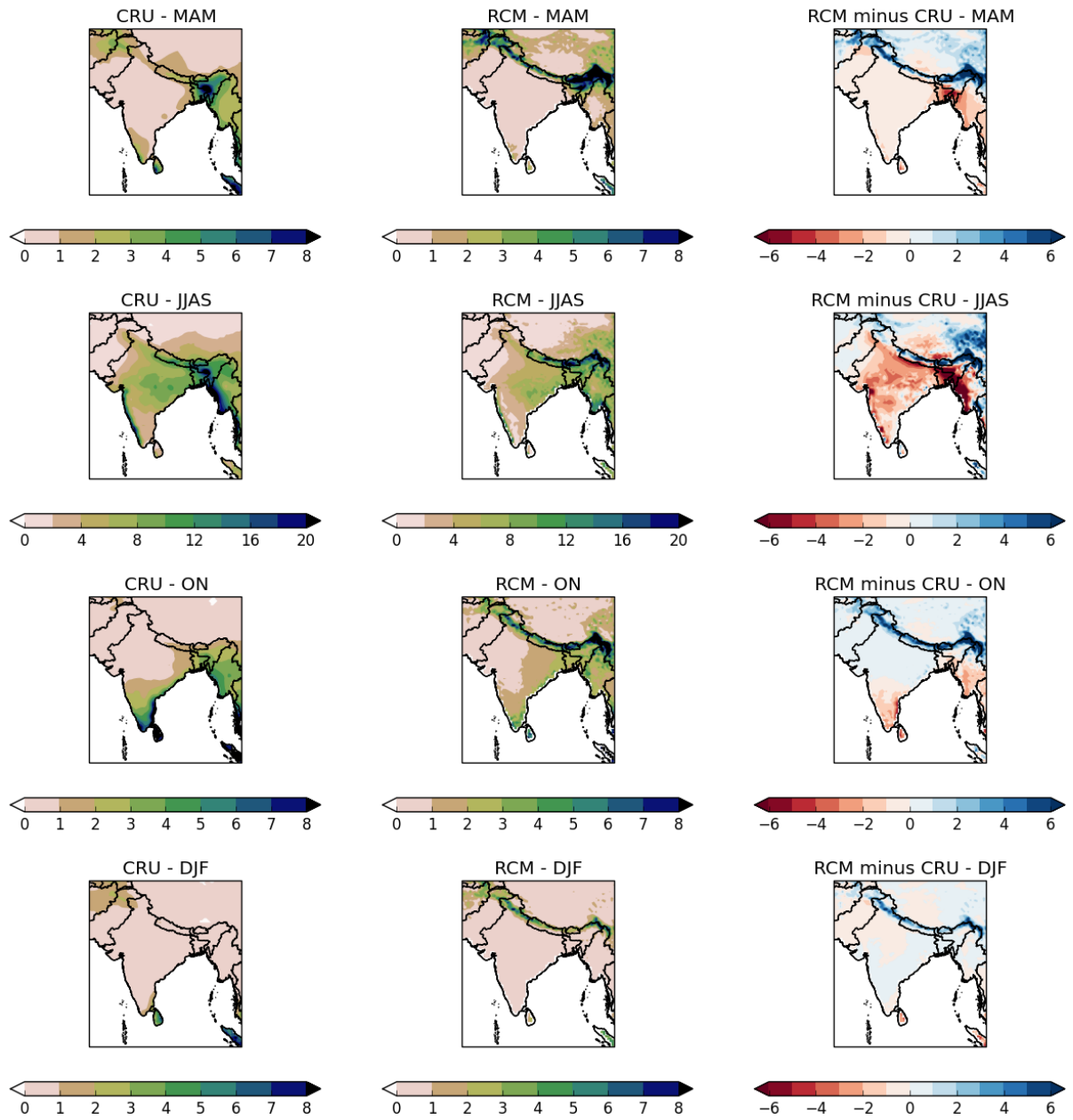


Figure 14: Maps of 1960-1999 climatological mean precipitation for March-May (MAM), June-September (JJAS), October-November (ON) and December-January (DJF) for the GFDL-CM3-forced RCM simulation and the CRU observational dataset. Differences between the RCM and CRU datasets are also shown.

4. Conclusion

Table 1 summarises the comparison of the output of the DECCMA RCM simulations with temperature and precipitation observations presented in this report for the GBM basin and northern India. The analysis reveals several common features of the three simulations:

1. The timing of warm and cool and wet and dry seasons is similar to that of observations, except that the maximum monthly precipitation is later in the year than in observations in the GFDL-CM3-forced simulation.
2. All three simulations have an overall cold bias for the region throughout most or all of the year. This is largest in winter, when all three simulations have cold biases across the entire region. However, the size of the cold bias varies between the simulations.
3. All three simulations have large local dry biases in Bangladesh and eastern India in the March-May season, with more extensive dry biases during the height of the summer monsoon (June-September). In the HadGEM2-ES-forced and GFDL-CM3-forced simulations these result in an overall dry bias for the region as a whole for these seasons.
4. In the Himalayas, in common with other HadRM3P simulations of the region (see Caesar et al., 2015), all three simulations have large cold and wet biases throughout the year. It is possible that these may be at least partially due to deficiencies in the observational datasets.

Simulation	Temperature	Precipitation
<i>RCM forced by HadGEM2-ES</i>	<p>Timing of warm and cool seasons similar to observations.</p> <p>Overall cold bias for the region throughout the year, except in May-Jun, largest in winter (~4°C in Jan mean temperature).</p> <p>Cold biases across the entire region in winter. Much smaller local cold biases during summer, with warm biases in some parts of northern India and Bangladesh. Large cold bias in Himalayas throughout the year.</p> <p>More extreme variation in temperature between winter and summer than in observations.</p>	<p>Timing of wet and dry seasons similar to observations.</p> <p>Overall dry bias for the region during wet months.</p> <p>Large local dry biases in Bangladesh and eastern India throughout Mar-Nov, with dry biases across most of the region in Jun-Sep.</p> <p>Wet bias in Himalayas throughout the year and to the west of the Mahanadi Delta in Jun-Sep.</p>
<i>RCM forced by CNRM-CM5</i>	<p>Timing of warm and cool seasons similar to observations.</p> <p>Overall cold bias for the region throughout the year, larger in winter than in summer (~1°C in monthly mean temperature in May-Jun, ~5°C in Jan mean temperature).</p> <p>Cold biases across the entire region throughout the year, except Mar-May, in which there are warm biases in Bangladesh and eastern India. Large cold bias in Himalayas throughout the year.</p> <p>More extreme variation in temperature between winter and summer than in observations.</p>	<p>Timing of wet and dry seasons similar to observations.</p> <p>Little overall bias for the region throughout the year.</p> <p>Large local dry biases in Bangladesh and eastern India in Mar-May, with more extensive dry biases in Jun-Sep.</p> <p>Wet bias in Himalayas throughout the year and across central India in Jun-Sep.</p>
<i>RCM forced by GFDL-CM3</i>	<p>Timing of warm and cool seasons similar to observations.</p> <p>Overall cold bias for the region throughout the year, except in Jun, largest in winter (~6°C in Jan mean temperature).</p> <p>Cold biases across the entire region in winter. Very small biases across most of the region during summer. Large cold bias in Himalayas throughout the year.</p> <p>Much more extreme variation in temperature between winter and summer than in observations.</p>	<p>Maximum monthly precipitation later in the year than in observations.</p> <p>Overall dry bias for the region during May-Aug.</p> <p>Large local dry biases in Bangladesh and eastern India in Mar-May, with dry biases across most of the region in Jun-Sep.</p> <p>Wet bias in Himalayas throughout the year.</p>

Table 1: Summary of a comparison of the output of the DECCMA RCM simulations for the GBM basin and northern India with temperature and precipitation observations.

This brief comparison of output from the DECCMA RCM simulations with observation is an initial validation of the simulations. It is designed to inform a broad range of potential users of the RCM output about some of the model biases that may be relevant to subsequent analysis of climate impacts. However, it has a number of limitations, which lead to recommendations for users of the simulation outputs (highlighted in bold type below):

1. The “biases” referred to in this document are differences between the output of the DECCMA RCM simulations and observational data. They are not strictly model biases as they are not solely due to deficiencies of the climate model simulations. Deficiencies in the observational datasets may also contribute. This is most likely to be the case for the large cold and wet biases reported for the topographically complex Himalayas. **Users of the RCM simulation outputs to whom these biases are relevant are encouraged to reassess model biases in this area after further investigating the deficiencies in the observational data.** Note, however, that differences between RCM output and climate observations may be more relevant to some users of the RCM output than model biases relative to the behaviour of the real world (e.g. where a numerical model used to assess climate impacts has been calibrated using climate observations).
2. The comparison with observations is confined to monthly and seasonal climatological means of temperature and precipitation. Other climate variables are known to be of interest to the DECCMA project (see Macadam, 2017 for a full listing of the climate variables provided to the project from the simulations), as are more subtle aspects of temperature and precipitation (e.g. extreme daily values). **Users of the RCM simulation outputs are encouraged to undertake their own analysis focussing on biases in the particular aspects of the climate that are relevant to their application of the data.**
3. This report relates to the ability of the RCM simulations to reproduce the observed climate of the 1960-1999 period. However, the simulations also cover whole of the 21st century. Although it is reasonable to assume that the 21st century portions of the simulations have biases broadly similar to those reported here for 1960-1999, this has not been established beyond doubt. Further work examining the mechanisms responsible for the biases, and how they may change in a warming climate, would be necessary to do so. **Users of the DECCMA RCM simulation outputs may reasonably assume that the biases**

described in this report apply throughout the full mid 20th century to end of 21st century simulation period, but should be aware that this is an assumption. This recommendation is consistent with the work of others that have attempted to statistically correct biases in RCM output for use in research on the impacts of future climate changes (e.g. Bennett et al., 2014).

4. The realism of the simulated future climate changes simulated by the RCM simulations is beyond the scope of this report. It is conceivable that there could be links between the simulation biases for the 1960-1999 period reported here and the realism of simulated future climate changes. However, establishing these for the DECCMA RCM simulations would require more detailed analysis of the simulations and a comprehensive assessment of the realism of the simulated future changes would likely require investigation of other simulation biases, including those in the GCMs that have been downscaled. Given this, **this report should not be used to make judgements on the realism of the future climate changes simulated by the different DECCMA RCM simulations, and the future climate changes simulated by the three simulations should be given equal weight in research on climate change impacts.**

5. Focussing on the interests of the DECCMA climate impacts community, this report has compared the DECCMA RCM simulation outputs with climate observations. It has not compared the RCM simulations outputs with the outputs of the forcing GCM simulations. It would be valuable to do so, however. In addition to verifying that the RCM simulations are consistent with their forcing GCM simulations on GCM-resolved spatial scales, it could contribute to assessing the value added to the GCM simulations by the finer-resolution RCM simulations. **In the absence of further work in this area, those using the RCM simulation outputs for research on climate change impacts are encouraged to consider the outputs of each GCM-RCM combination as those of a single climate model entity and not seek to attribute results to the behaviour of either the GCM or RCM components of the model configuration.**

Acknowledgements

We thank our Met Office colleagues Florian Gallo, Simon Tucker, Simon Wilson, Saeed Sadri and David Hein for assistance with the HadRM3P RCM simulations and Erasmo Buonomo and Richard Jones for reviewing this document.

We acknowledge the World Climate Research Programme's Working Group on Coupled Modelling, which is responsible for CMIP, and we thank the climate modelling groups at the Met Office Hadley Centre, the Centre National de Recherches Météorologiques / Centre Européen de Recherche et Formation Avancée en Calcul Scientifique and the NOAA Geophysical Fluid Dynamics Laboratory for producing and making available their model output. For CMIP the US Department of Energy's Program for Climate Model Diagnosis and Intercomparison provides coordinating support and led development of software infrastructure in partnership with the Global Organization for Earth System Science Portals.

This work was carried out under the Deltas, vulnerability and Climate Change: Migration and Adaptation (DECCMA) project (IDRC 107642) under the Collaborative Adaptation Research Initiative in Africa and Asia (CARIAA) programme with financial support from the UK Government's Department for international Development (DFID) and the International Development Research Centre (IDRC), Canada. The views expressed in this work are those of the creators and do not necessarily represent those of DFID and IDRC or its Boards of Governors.

References

Adler, R.F. et al. (2003), "The Version 2 Global Precipitation Climatology Project (GPCP) Monthly Precipitation Analysis (1979-Present)", *J. Hydrometeor.*, Vol. 4, pp. 1147-1167, [http://dx.doi.org/10.1175/1525-7541\(2003\)004<1147:TVGPCP>2.0.CO;2](http://dx.doi.org/10.1175/1525-7541(2003)004<1147:TVGPCP>2.0.CO;2)

Bennett, J.C. et al. (2014), "Performance of an empirical bias-correction of a high-resolution climate dataset", *Int. J. Climatol.*, Vol. 34, pp. 2189–2204, <http://dx.doi.org/10.1002/joc.3830>.

Caesar, J. et al. (2015), "Temperature and precipitation projections over Bangladesh and the upstream Ganges, Brahmaputra and Meghna systems", *Environ. Sci.: Processes Impacts*, Vol. 17, pp. 1047-1056, <http://dx.doi.org/10.1039/c4em00650j>.

Harris, I. et al. (2014), "Updated high-resolution grids of monthly climatic observations – the CRU TS3.10 Dataset", *Int. J. Climatol.*, Vol. 34, pp. 623–642, <http://dx.doi.org/10.1002/joc.3711>.

Herold, N. et al. (2016), "How much does it rain over land?", *Geophys. Res. Lett.*, Vol. 43, pp. 341–348, <http://dx.doi.org/10.1002/2015GL066615>.

Janes, T., I. Macadam (2017), "Selection of climate model simulations for the DECCMA project", DECCMA Working Paper, Deltas, Vulnerability and Climate Change: Migration and Adaptation, IDRC Project Number 107642, www.deccma.com.

Macadam, I. (2017), "Climate data for DECCMA: Description, format, available variables", Met Office report for the DECCMA project, http://www.geodata.soton.ac.uk/deccma/download/DECCMA_Climate_Data_Description_20170425.pdf.

Taylor, K., R. Stouffer, G. Meehl (2012), "An Overview of CMIP5 and the experiment design", *Bull. Amer. Meteor. Soc.*, Vol. 93/4, pp. 485-498, <http://dx.doi.org/10.1175/BAMS-D-11-00094.1>

Weedon, G.P., et al. (2010), "The WATCH forcing data 1958-2001: A meteorological forcing dataset for land surface and hydrological models", WATCH Technical Report No. 22.

Willmott, C.J., K. Matsuura (1995), "Smart Interpolation of Annually Averaged Air Temperature in the United States", *J. Appl. Meteor.*, Vol. 34, pp. 2577–2586, [http://dx.doi.org/10.1175/1520-0450\(1995\)034<2577:SIOAAA>2.0.CO;2](http://dx.doi.org/10.1175/1520-0450(1995)034<2577:SIOAAA>2.0.CO;2)

Xie, P., P.A. Arkin (1997), "Global precipitation: A 17-year monthly analysis based on gauge observations, satellite estimates, and numerical model outputs", *Bull. Amer. Meteor. Soc.*, Vol. 78, pp. 2539 – 2558, [http://dx.doi.org/10.1175/1520-0477\(1997\)078<2539:GPAYMA>2.0.CO;2](http://dx.doi.org/10.1175/1520-0477(1997)078<2539:GPAYMA>2.0.CO;2)

Yatagai, A. et al. (2009), "A 44-Year Daily Gridded Precipitation Dataset for Asia Based on a Dense Network of Rain Gauges", *SOLA*, Vol. 5, pp. 137-140, <http://doi.org/10.2151/sola.2009-035>

Met Office
FitzRoy Road, Exeter
Devon EX1 3PB
United Kingdom

Tel (UK): 0370 900 0100 (Int): +44 1392 885680
Fax (UK): 0370 900 5050 (Int): +44 1392 885681
enquiries@metoffice.gov.uk
www.metoffice.gov.uk